A theoretical investigation of ferromagnetic tunnel junctions with 4-valued conductances

2003 J. Phys.: Condens. Matter 15 8797

(http://iopscience.iop.org/0953-8984/15/50/012)

INSTITUTE OF PHYSICS PUBLISHING JOURNAL OF PHYSICS: CONDENSED MATTER

J. Phys.: Condens. Matter **15** (2003) 8797–8804 PII: S0953-8984(03)67070-0

A theoretical investigation of ferromagnetic tunnel junctions with 4-valued conductances

Satoshi Kokado[1] **and Kikuo Harigaya**[1,2]

[1] Nanotechnology Research Institute, AIST, Tsukuba 305-8568, Japan
[2] Synthetic Nano-Function Materials Project, AIST, Tsukuba 305-8568, Japan

E-mail: satoshi-kokado@aist.go.jp and k.harigaya@aist.go.jp

Received 4 August 2003
Published 3 December 2003
Online at stacks.iop.org/JPhysCM/15/8797

Abstract

In considering a novel function in ferromagnetic tunnel junctions consisting of ferromagnet (FM)/barrier/FM junctions, we have theoretically investigated the multiple-valued (or multi-level) cell property, which is in principle realized by sensing the conductances of four states recorded with magnetization configurations of two FMs; that is, (up, up), (up, down), (down, up), (down, down). To obtain such 4-valued conductances, we propose FM1/spin-polarized barrier/FM2 junctions, where FM1 and FM2 are different ferromagnets, and the barrier has spin dependence. The proposed idea is applied to the case of the barrier having localized spins. Assuming that all the localized spins are pinned parallel to the magnetization axes of FM1 and FM2, 4-valued conductances are explicitly obtained for the case of many localized spins. Furthermore, objectives for an ideal spin-polarized barrier are discussed.

1. Introduction

Ferromagnetic tunnel junctions (FTJ) such as ferromagnet (FM)/barrier/FM junctions [1–4] have been recently applied to elements in magnetic random access memories (MRAM) because of their tunnel magnetoresistance (TMR) effect, which appears when an applied magnetic field changes the angle between the magnetizations of two FMs. In practical use, a spin-valve type [5] is usually adopted. For the writing process, the magnetization of only one side of the FM is changed under the applied field, so the magnetization configurations between the two FMs are parallel (P) or anti-parallel (AP); for the reading process, the difference in resistance between the P and AP cases is used.

For the FTJ, much effort has been made to increase the TMR ratio, which is defined by $(\Gamma_{\mathrm{P}} - \Gamma_{\mathrm{AP}})/\Gamma_{\mathrm{AP}}$, where $\Gamma_{\mathrm{P(AP)}}$ is conductance of the P (AP) case. Experimentally, the TMR ratio of Co–Fe/Al–O/Co–Fe junctions reached 60% at room temperature [2] in investigations of the influence of the fabrication method for oxide barrier on the TMR effect, epitaxially grown $Ga_{1-x}Mn_xAs/AlAs/Ga_{1-x}Mn_xAs$ junctions have exhibited a TMR ratio more than 70% at

8 K [3], and the TMR ratio of Co/Fe-doped Al_2O_3/$Ni_{80}Fe_{20}$ junctions has been successfully enhanced compared to those with undoped Al_2O_3 [4]. Theoretically, the TMR ratio for epitaxial Fe/MgO/Fe(001) junctions became more than 300% because of coherent tunnelling with conservation of intralayer momentum [6], and TMR ratios for junctions having a sheet with 100% spin polarized dopants in the barrier [7] and the Fe-doped barrier [8] were enhanced because of spin polarization of resonant states inside the barrier and spin dependent energy levels inside it, respectively. Furthermore, double barrier junctions of FM/barrier/nonmagnetic layer/barrier/FM reached a TMR ratio of more than 5000% at a specific thickness of the nonmagnetic layer, as a result of spin dependent conduction through resonant levels in the layer [9].

By comparing such FTJ with elements [10] in other memories such as Flash memory [11], however, we find out that there are few studies on the multiple-valued (or multi-level) cell property [11], which allows many bits to be stored in each memory cell, and reduces the memory cell size by 1/(the number of bits). If such a property is included in the FTJ, they will function as a more efficient memory cell than the conventional one.

In this paper, we theoretically investigate the multiple-valued cell property [11] in the FTJ. In a possible scheme, the recorded states are supposed to be four magnetization configurations of two FMs consisting of (up, up), (up, down), (down, up), (down, down), which are obtained by applying magnetic fields to respective FMs. The FTJ correspond to 2 bits memory cells. Then, in order to sense all the states, 4-valued conductances corresponding to the respective states are obviously necessary. By paying attention to the magnitude of total magnetization in the whole system, a model to obtain such conductances is considered to be FM1/spin-polarized barrier (SPB)/FM2 junctions, where the FM1 and FM2 have different spin polarizations, and magnetization in the barrier is pinned, according to the following procedure. First, a difference of conductances between (up, up) and (down, down) will appear, if the barrier is a SPB. Second, a difference between (up, down) and (down, up) will be obtained by introducing FM1 and FM2, in addition to the SPB. In actual calculations, the junctions exhibit 4-valued conductances. Further, the proposed idea is applied to the case of the barrier having localized spins. When all the localized spins are pinned parallel to the magnetization axes of FM1 and FM2, 4-valued conductances are explicitly obtained in the case of many localized spins. Finally, objectives for an ideal SPB to certainly observe such conductances are discussed.

2. 3-valued and 4-valued conductances

We first investigate the conductance of the FM1/SPB/FM2 junctions, where the barrier merely has spin dependent height due to the pinned magnetization, and its material is not specified for general discussions. To simply find the intrinsic properties, one-dimensional systems are adopted. Within the Green function technique [12, 13], the conductance is given by

$$\Gamma = \frac{4\pi^2 e^2}{h} \sum_{\sigma=\uparrow,\downarrow} \sum_{\sigma'=\uparrow,\downarrow} T_{\sigma,\sigma'} D_{1,\sigma}(E_{\mathrm{F}}) D_{2,\sigma'}(E_{\mathrm{F}}), \tag{1}$$

where σ is spin of a tunnel electron, and $D_{1(2),\sigma}(E)$ denotes the local density-of-states (DOS) at an interfacial layer in FM1(2) at the Fermi level, E_{F}. $T_{\sigma,\sigma'}$ is a spin dependent transmission coefficient including the spin-flip process of $\sigma \neq \sigma'$, and is proportional to $|G_{\sigma,\sigma'}|^2$, where $G_{\sigma,\sigma'}$ is the (σ, σ') component of an element between both edge sites in the barrier for the Green function of the whole system [12, 13]. As the barrier height becomes higher, $T_{\sigma,\sigma'}$ decreases.

Using equation (1), we obtain conductances for respective configurations, where the magnetization state of FM1 (FM2) is represented by m1 (m2), which is $\Uparrow$ or $\Downarrow$. By introducing $\gamma_{\mathrm{m1,m2}} = \Gamma_{\mathrm{m1,m2}} / \Gamma_{\Uparrow,\Uparrow}$, we have

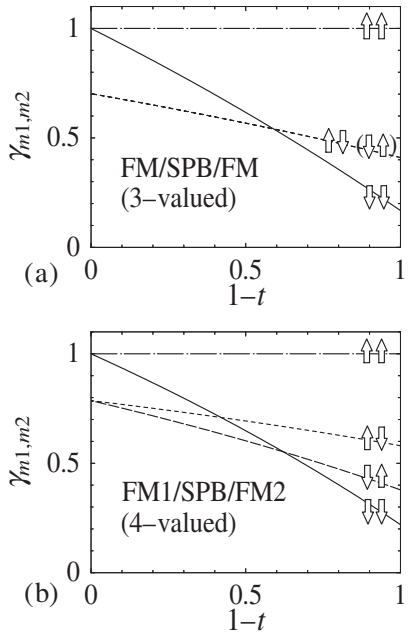

Figure 1. $\gamma_{\mathrm{m1,m2}}$ versus $1-t$ $[=(T_{\Uparrow,\Uparrow}-T_{\Downarrow,\Downarrow})/T_{\Uparrow,\Uparrow}]$ for $t'=t''=0$. (a) The FM/spin-polarized barrier (SPB)/FM junctions with 3-valued conductances. $(d_1,d_2)=(0.41,0.41)$. (b) The FM1/SPB/FM2 junctions with 4-valued conductances, where FM1 and FM2 have different local DOSs at E_{F}. $(d_1,d_2)=(0.38,0.58)$. Here, sets of two arrows represent the magnetization configurations of two FMs.

$$\gamma_{\Uparrow,\Uparrow}=\frac{\Gamma_{\Uparrow,\Uparrow}}{\Gamma_{\Uparrow,\Uparrow}}=1, \tag{2}$$

$$\gamma_{\Downarrow,\Downarrow}=\frac{\Gamma_{\Downarrow,\Downarrow}}{\Gamma_{\Uparrow,\Uparrow}}=\frac{d_1d_2+t+t'd_2+t''d_1}{1+td_1d_2+t'd_2+t''d_1}, \tag{3}$$

$$\gamma_{\Uparrow,\Downarrow}=\frac{\Gamma_{\Uparrow,\Downarrow}}{\Gamma_{\Uparrow,\Uparrow}}=\frac{d_2+td_1+t'+t''d_1d_2}{1+td_1d_2+t'd_2+t''d_1}, \tag{4}$$

$$\gamma_{\Downarrow,\Uparrow}=\frac{\Gamma_{\Downarrow,\Uparrow}}{\Gamma_{\Uparrow,\Uparrow}}=\frac{d_1+td_2+t'd_1d_2+t''}{1+td_1d_2+t'd_2+t''d_1}, \tag{5}$$

with $t=T_{\downarrow,\downarrow}/T_{\uparrow,\uparrow}$, $t'=T_{\uparrow,\downarrow}/T_{\uparrow,\uparrow}$, $t''=T_{\downarrow,\uparrow}/T_{\uparrow,\uparrow}$, $d_1=D_{1,\mathrm{m}}(E_{\mathrm{F}})/D_{1,\mathrm{M}}(E_{\mathrm{F}})$, and $d_2=D_{2,\mathrm{m}}(E_{\mathrm{F}})/D_{2,\mathrm{M}}(E_{\mathrm{F}})$, where $D_{1(2),\mathrm{M}}(E_{\mathrm{F}})$ and $D_{1(2),\mathrm{m}}(E_{\mathrm{F}})$ correspond to local DOSs at E_{F} for majority spin and for minority spin of the case of $\Uparrow$, $\Uparrow$, respectively. In addition, the relation of $0\leqslant d_1,d_2\leqslant 1$ is satisfied. Note here that the case of $t=1$ and $t'=t''=0$ has 2-valued conductances, and then $1-\gamma_{\Uparrow,\Downarrow}$ (or $1-\gamma_{\Downarrow,\Uparrow}$) results in the Julliere model [14].

By putting $t'=t''=0$, we investigate the $1-t$ $[=(T_{\uparrow,\uparrow}-T_{\downarrow,\downarrow})/T_{\uparrow,\uparrow}]$ dependence of $\gamma_{\mathrm{m1,m2}}$. In particular, we study the influence on $\gamma_{\mathrm{m1,m2}}$ of a change from the non-spin-polarized barrier to the spin-polarized one.

The FM/SPB/FM junctions with $d_1=d_2$ and $t\neq d_1$ exhibit 3-valued conductances, while those with $t=d_1$ have 2-valued conductances. Figure 1(a) shows $\gamma_{\mathrm{m1,m2}}$ with $d_1=d_2=0.41$ [15][3], which are determined by the least squares method such that $(\gamma_{\Uparrow,\Downarrow},\ \gamma_{\Downarrow,\Downarrow})$ becomes $(0.55,0.1)$ at $1-t=1$. The quantities $\gamma_{\Downarrow,\Downarrow}$ and $\gamma_{\Uparrow,\Downarrow}$ decrease nearly linearly

[3] Materials with $d_1=d_2=0.41$ and $d_1=0.38$ correspond nearly to Co, Fe, and $Ni_{80}Fe_{20}$, while $d_2=0.58$ is Ni.

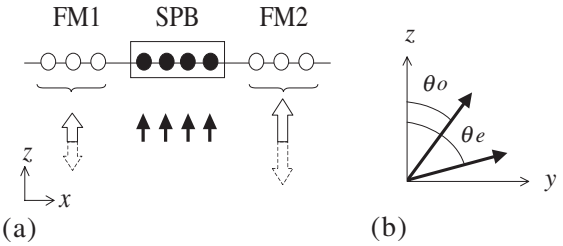

Figure 2. (a) A schematic illustration of the FM1/SPB/FM2 junctions, where localized spins are linearly configured in the barrier. Open (solid) arrays represent the FM's magnetizations (localized spins). (b) Configurations of the localized spins projected in the yz-plane. $\theta_{\rm o}$ ($\theta_{\rm e}$) is the angle at odd (even) sites between the localized spins and the z-axis.

with increasing $1-t$, while $\gamma_{\Downarrow,\Downarrow}$ crosses $\gamma_{\Uparrow,\Downarrow}$ at $1-t=1-d_1$, and $\gamma_{\Downarrow,\Downarrow}$ is smaller than $\gamma_{\Uparrow,\Downarrow}$ for $1-t>1-d_1$. The differences of $\gamma_{\rm m1,m2}$ between all the configurations become large near $1-t=1$.

The FM1/SPB/FM2 junctions with $d_1<d_2$ and $t\neq d_1, d_2$ exhibit 4-valued conductances, while those with $t=d_1$ or d_2 have 3-valued conductances. Figure 1(b) shows $\gamma_{\rm m1,m2}$ with $d_1=0.38$ and $d_2=0.58$ [15] (see footnote 3), which is determined by the least squares method such that ($\gamma_{\Uparrow,\Downarrow}$, $\gamma_{\Downarrow,\Uparrow}$, $\gamma_{\Downarrow,\Downarrow}$) becomes (0.7, 0.4, 0.1) at $1-t=1$. The quantities $\gamma_{\Downarrow,\Downarrow}$, $\gamma_{\Uparrow,\Downarrow}$, and $\gamma_{\Downarrow,\Uparrow}$ decrease with $1-t$, while $\gamma_{\Downarrow,\Downarrow}$ crosses $\gamma_{\Uparrow,\Downarrow}$ at $1-t=1-d_2$ and $\gamma_{\Downarrow,\Uparrow}$ at $1-t=1-d_1$. The differences between all $\gamma_{\rm m1,m2}$ are obviously found near $1-t=1$.

3. Application to a barrier having localized spins

As an example to obtain $T_{\sigma,\sigma'}$ definitively, we focus on the barrier having localized spins due to magnetic ions, or ions in magnetic particles which are configured linearly and with the same interval (see figure 2(a)). We investigate $\gamma_{\rm m1,m2}$ through a quantum well potential structure with dependence on spin by assuming that the potential of the conduction level at the magnetic ion site is lower than that in the original barrier part, and magnetic couplings between the localized spins and the magnetizations in the FMs are so small that their influence on the spin dependent conduction might be negligible. We use a single orbital tight-binding model with nearest neighbour transfer integrals, and take into account exchange interactions between the tunnel electron spin and localized spins [8], while couplings between localized spins are not specified because their ferromagnetic, antiferromagnetic, and canted states are considered. In the unit of magnitudes of the transfer integral, the Hamiltonian in the barrier is given by

$$\mathcal{H}=e\sum_{i,\sigma}|i,\sigma\rangle\langle i,\sigma|-\sum_{i,\sigma}(|i,\sigma\rangle\langle i+1,\sigma|+\text{h.c.})-J\sum_{i,\sigma,\sigma'}\boldsymbol{\sigma}_{\sigma,\sigma'}\cdot\mathbf{S}_i|i,\sigma\rangle\langle i,\sigma'|, \tag{6}$$

where $|i,\sigma\rangle$ is an orbital with spin-σ ($=\uparrow$ or $\downarrow$) at the ith site, and e denotes the on-site energy. Further, J is a ferromagnetic exchange integral with positive sign [8], $\boldsymbol{\sigma}_{\sigma,\sigma'}$ is the (σ,σ') component of the Pauli matrix, and $\mathbf{S}_i$ [$=(S_{i,x}, S_{i,y}, S_{i,z})$] is regarded as a classical spin at the ith site.

When the number of localized spins is n (>1), $T_{\sigma,\sigma'}$ is proportional to $|\langle 1,\sigma|G|n,\sigma'\rangle|^2$, where G is treated approximately as a bare Green function only in the barrier on the assumption that the self energy correction is negligibly small, reflecting very small couplings between the FMs and the SPB. Using equation (6), G is written as

$$G=(\mathcal{G}^{-1}-\mathcal{T})^{-1}, \tag{7}$$

with $\mathcal{T} = -\sum_{i,\sigma}(|i,\sigma\rangle\langle i+1,\sigma| + \text{h.c.})$, and

$$\mathcal{G} = \left[(E_{\rm F} - e + \mathrm{i}0^+)\sum_{i,\sigma}|i,\sigma\rangle\langle i,\sigma| + J\sum_{i,\sigma,\sigma'}\boldsymbol{\sigma}_{\sigma,\sigma'}\cdot\mathbf{S}_i|i,\sigma\rangle\langle i,\sigma'|\right]^{-1}. \tag{8}$$

Here, $\mathcal{G}$ is a Green function on sites unconnected to the other sites, and is exactly expressed as

$$\mathcal{G} = \sum_{i,\sigma,\sigma'}\mathcal{G}_i^{(\sigma,\sigma')}|i,\sigma\rangle\langle i,\sigma'|, \tag{9}$$

with

$$\mathcal{G}_i^{(\sigma,\sigma')} = \frac{g^{-1}\delta_{\sigma,\sigma'} - J\boldsymbol{\sigma}_{\sigma,\sigma'}\cdot\mathbf{S}_i}{g^{-2} - J^2S^2} = \frac{1}{2}\left(\delta_{\sigma,\sigma'} + \frac{\boldsymbol{\sigma}_{\sigma,\sigma'}\cdot\mathbf{S}_i}{S}\right)\frac{1}{g^{-1}+JS} + \frac{1}{2}\left(\delta_{\sigma,\sigma'} - \frac{\boldsymbol{\sigma}_{\sigma,\sigma'}\cdot\mathbf{S}_i}{S}\right)\frac{1}{g^{-1}-JS}, \tag{10}$$

$g = (E_{\rm F} - e + \mathrm{i}0^+)^{-1}$, and $\mathbf{S}_i^2 = S^2$. The first and second terms correspond to components of a lower level with $e - JS$ and of an upper level with $e + JS$, respectively. For $J = 0$, $\mathcal{G}_i^{(\sigma,\sigma')}$ certainly has the non-spin-polarized feature. For $J \neq 0$, when $\mathbf{S}_i$ is along the quantum axis, i.e., $\boldsymbol{\sigma}_i\cdot\mathbf{S}_i/S = \sigma_{i,z}$, $\mathcal{G}_i^{(\sigma,\sigma')}$ has only a spin-up (-down) component for the lower (upper) level, which represents the largely spin-polarized feature, while when $\mathbf{S}_i$ perpendicular to the quantum axis, $\mathcal{G}_i^{(\sigma,\sigma')}$ shows no difference between spin-up and spin-down in both levels, which represents the non-spin-polarized feature.

In this calculation, we utilize the same set $(d_1, d_2) = (0.38, 0.58)$ as above, and choose $e - E_{\rm F} = 3.5$, where a condition of $e - JS > E_{\rm F}$ is used, based on strong on-site Coulomb repulsions at magnetic ion sites [8]. Further, localized spins are assumed to exist parallel to the yz-plane, and the angle at odd (even) sites between the localized spins and the z-axis is written as $\theta_{\rm o}$ ($\theta_{\rm e}$) (see figure 2(b)).

In figure 3(a), we show the JS dependence of $\gamma_{\rm m1,m2}$ for $\theta_{\rm o}/\pi = \theta_{\rm e}/\pi = 0$. At $JS = 0$, the difference of $\gamma_{\rm m1,m2}$ exists only between the P and AP cases. With increasing JS, each $\gamma_{\rm m1,m2}$ approaches its saturation value, which corresponds just to each $\gamma_{\rm m1,m2}$ at $1 - t = 1$ shown in figure 1(b). It is worth noting that each $\gamma_{\rm m1,m2}$ of $n = 8$ saturates more rapidly than that of $n = 2$. Such behaviour reflects the fact that t of $n = 8$ decreases with JS more drastically than that of $n = 2$ according to

$$t = \frac{\sinh^2\kappa_\downarrow/\sinh^2[\kappa_\downarrow(n+1)]}{\sinh^2\kappa_\uparrow/\sinh^2[\kappa_\uparrow(n+1)]}, \tag{11}$$

with $2\cosh\kappa_{\uparrow(\downarrow)} = e-(+)JS - E_{\rm F}$ [16, 13]. When the decay exponentials in the hyperbolic sine of equation (11) can be neglected owing to large $\kappa_{\uparrow(\downarrow)}$, we have $t \approx \mathrm{e}^{-2\Delta\kappa n}$, where $\Delta\kappa$, defined by $\kappa_\downarrow - \kappa_\uparrow$, increases with JS [17].

Figure 3(b) shows the $\theta_{\rm o}$ ($=\theta_{\rm e}$) dependence of $\gamma_{\rm m1,m2}$ for $JS = 1$. A condition of $\theta_{\rm o}/\pi = -0.5$ (0) represents localized spins oriented in the $-y$ (z) direction. At $\theta_{\rm o}/\pi = -0.5$, only the difference between the P and AP cases is present. The difference at $\theta_{\rm o}/\pi = -0.5$ of $n = 8$ is much smaller than that of $n = 2$, because the spin-flip tunnelling process increases owing to an increase of the transverse components of the localized spins. As $\theta_{\rm o}$ approaches 0, differences of $\gamma_{\rm m1,m2}$ between all the configurations become large.

In figure 3(c), we investigate the $\theta_{\rm o}$ dependence of $\gamma_{\rm m1,m2}$ for $JS = 1$ and $\theta_{\rm e}/\pi = 0$. The change of $\theta_{\rm o}$ from $-\pi$ to 0 corresponds to that from the antiferromagnetic state to the ferromagnetic one via canted ones. The quantity $\gamma_{\rm m1,m2}$ exhibits a difference only between the P and AP cases at $\theta_{\rm o}/\pi = -1$; they behave individually for $-1 < \theta_{\rm o}/\pi < 0$; and there are large differences between all the configurations at $\theta_{\rm o}/\pi = 0$.

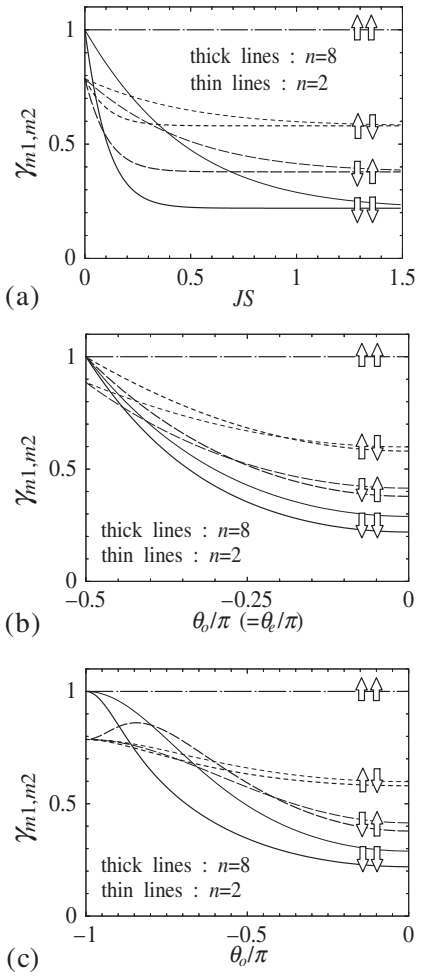

Figure 3. $\gamma_{\mathrm{m1,m2}}$ of the FTJ in figure 2. $(d_1, d_2) = (0.38, 0.58)$. The notation follows that in figure 1. (a) JS dependence up to $JS = 1.49$ for $\theta_{\mathrm{o}} = \theta_{\mathrm{e}} = 0$. (b) θ_{o} $(= \theta_{\mathrm{e}})$ dependence for $JS = 1$. (c) θ_{o} dependence for $JS = 1$ and $\theta_{\mathrm{e}} = 0$. Here, the unit of J is the magnitude of the transfer integral.

4. Discussions

We now comment on a comparison with previous work. As far as we are aware, resistance versus magnetic fields observed for Co/Fe-doped $Al_2O_3/Ni_{80}Fe_{20}$ junctions [4], which may be similar to FM1/SPB/FM2 junctions with the above-mentioned barrier having localized spins, have not confirmed 3-valued or 4-valued conductances. Note that localized spins of Fe were not pinned, and $1 - t$ might possibly be small. On the other hand, the observed enhancement of several per cent in the TMR ratio appears to originate from the behaviour of $\gamma_{\Uparrow,\Downarrow}$ or $\gamma_{\Downarrow,\Uparrow}$ for $1 - t \neq 0$, as shown in figure 1. Also, the increase of the TMR ratio with JS shown in figure 3(a) agrees qualitatively with that of the previous theoretical study [8].

We here consider an ideal SPB to certainly observe 3-valued or 4-valued conductances. For a barrier having magnetic particles, we have two objectives, which are

(i) to strongly pin the magnetization of magnetic particles in the barrier parallel to the magnetization axes of the FMs, and

(ii) to diminish the magnetic couplings between the magnetic particles and the FMs.

As for (i), we propose magnetic particles having a coercive field higher than those of the FMs. Also, it may be effective to apply exchange bias from an antiferromagnet [5] to the magnetic particles. Here, the antiferromagnet is located not between the FMs and the SPB but at the side of the SPB in the FTJ, meaning that few conduction electrons may flow in the antiferromagnet because it is not connected to FM electrodes. For (ii), we suppose that distances between magnetic particles and FMs should be well controlled so that the magnetic dipole–dipole interactions between them become very small and have little influence on the spin dependent conduction.

As a realistic SPB, which could satisfy such objectives, we consider a carbon nanotube encapsulating magnetic particles [18, 19] for the following reasons. The size of the magnetic particles may be made close to that of a single domain particle by tuning the conditions of fabrication. Note that the coercive field was recently observed as about 0.5 kOe at 300 K even for Fe particles encapsulated with non-single domain size of about 70 nm [18]. Further, magnetic particles can be encapsulated not only at edges of the nanotube [18] but also in the inner region [20], where distances between the particles and the edges may be tunable by controlling nanotube growth processes. It is also mentioned that the nanotube itself has very long spin-flip scattering lengths which extend at least 130 nm [21].

As another SPB, we propose a ferromagnetic barrier such as EuS, where bulk EuS has a band gap of 1.65 eV and an exchange splitting of the conduction band of 0.36 eV [22]. In fact, it has been shown experimentally that the EuS tunnel barrier can be used as a highly efficient spin filter [23], and it has been theoretically found that the ferromagnetic barrier largely contributes to an increase of the TMR ratio in double ferromagnetic barrier junctions, where external and central electrodes are nonmagnetic [9, 24, 25]. When such a ferromagnetic barrier is used as the SPB, we design FM1/barrier/SPB/barrier/FM2 junctions, where the antiferromagnet may be layered at the side of the SPB in order to pin the magnetization of the SPB strongly.

From the viewpoint of device applications, we anticipate that 2 bits/cell MRAM will be realized using 4-valued conductances. At the same time, we mention that the FTJ with magnetization reversals between $\Uparrow$, $\Uparrow$ and $\Downarrow$, $\Downarrow$ show larger TMR ratio compared with the conventional spin-valve type [5], in the case of a largely spin-polarized barrier.

5. Conclusion

We have theoretically investigated the multiple-valued cell property, which is in principle realized by sensing three or four states recorded with magnetization configurations of two FMs. The FM/SPB/FM junctions have 3-valued conductances to sense three states, and the FM1/SPB/FM2 junctions, where FM1 and FM2 have different local DOSs at E_F, have 4-valued conductances to sense four states. When the barrier has localized spins, differences among those conductances are strongly influenced by the magnitude of the interaction between the tunnel electron spin and localized spins, and the directions of the localized spins. In the case of many localized spins, respective conductances rapidly approach saturation values. Further, objectives for the ideal SPB to observe such conductances have been given and considered. We expect that the present proposal on 4-valued conductances will contribute a great deal to the realization of 2 bits/cell MRAM in the near future.

Acknowledgments

This work has been supported by Special Coordination Funds for Promoting Science and Technology, Japan. One of the authors (KH) acknowledges partial financial support from NEDO via Synthetic Nano-Function Materials Project, AIST, Japan, too.

References

[1] Miyazaki T and Tezuka N 1995 *J. Magn. Magn. Mater.* **139** L231
Moodera J S, Kinder L R, Wong T M and Meservey R 1995 *Phys. Rev. Lett.* **74** 3273
[2] Tsunoda M, Nishikawa K, Ogata S and Takahashi M 2002 *Appl. Phys. Lett.* **80** 3135
[3] Tanaka M and Higo Y 2001 *Phys. Rev. Lett.* **87** 026602
[4] Jansen R and Moodera J S 1999 *Appl. Phys. Lett.* **75** 400
[5] Parkin S S, Roche K P, Samant M G, Rice P M, Beyers R B, Scheuerlein R E, O'Sullivan E J, Brown S L, Bucchigano J, Abraham D W, Lu Yu, Rooks M, Trouilloud P L, Wanner R A and Gallagher W J 1999 *J. Appl. Phys.* **85** 5828
[6] Mathon J and Umerski A 2001 *Phys. Rev.* B **63** 220403(R)
[7] Jansen R and Lodder J C 2000 *Phys. Rev.* B **61** 5860
[8] Inoue J, Nishimura N and Itoh H 2002 *Phys. Rev.* B **65** 104433
[9] Wilczynski M and Barnas J 2001 *Sensors Actuators* A **91** 188
[10] For example, see Takahashi N, Ishikuro H and Hiramoto T 2000 *Appl. Phys. Lett.* **76** 209
[11] Giridhar R V 1996 *Japan. J. Appl. Phys.* **35** 6347
[12] Todorov T N, Briggs G A D and Sutton A P 1993 *J. Phys.: Condens. Matter* **5** 2389
[13] Kokado S, Ichimura M, Onogi T, Sakuma A, Arai R, Hayakawa J, Ito K and Suzuki Y 2001 *Appl. Phys. Lett.* **79** 3986
[14] Julliere M 1975 *Phys. Lett.* A **54** 225
[15] Moodera J S and Mathon G 1999 *J. Magn. Magn. Mater.* **200** 248
[16] Sutton A P, Finnist M W, Pettifor D G and Ohta Y 1988 *J. Phys. C: Solid State Phys.* **21** 35
[17] For example, see Mathon J 1997 *Phys. Rev.* B **56** 11810
[18] Zhang X X, Wen G H, Huang S, Dai L, Gao R and Wang Z L 2001 *J. Magn. Magn. Mater.* **231** L9
[19] Kokado S and Harigaya K 2004 *Physica* E at press
[20] Zhao X, Inoue S, Jinno M, Suzuki T and Ando Y 2003 *Chem. Phys. Lett.* **373** 266
[21] Tsukagoshi K, Alphenaar B W and Ago H 1999 *Nature* **401** 572
[22] Hao X, Moodera J S and Meservey R 1990 *Phys. Rev.* B **42** 8235
[23] LeClair P, Ha J K, Swagten H J M, Kohlhepp J T, van de Vin C H and de Jonge W J M 2002 *Appl. Phys. Lett.* **80** 625
[24] Filip A T, LeClair P, Smits C J P, Kohlhepp J T, Swagten H J M, Koopmans B and de Jonge W J M 2002 *Appl. Phys. Lett.* **81** 1815
[25] Wilczyński M, Barnaś J and Świrkowicz R 2003 *Phys. Status Solidi* a **196** 109